

# The Origin of the High Conductivity of Poly(3,4-ethylenedioxythiophene)–Poly(styrenesulfonate) (PEDOT–PSS) Plastic Electrodes

X. Crispin,<sup>\*,†</sup> F. L. E. Jakobsson,<sup>†</sup> A. Crispin,<sup>‡</sup> P. C. M. Grim,<sup>§</sup> P. Andersson,<sup>†</sup> A. Volodin,<sup>||</sup> C. van Haesendonck,<sup>||</sup> M. Van der Auweraer,<sup>§</sup> W. R. Salaneck,<sup>‡</sup> and M. Berggren<sup>†</sup>

Department of Science and Technology, Campus Norrköping, Linköping University, S-60174 Norrköping, Sweden, Department of Physics and Measurement Technology, Linköping University, S-58183 Linköping, Sweden, Division of Molecular and NanoMaterials, Katholieke Universiteit Leuven, Celestijnenlaan 200F, B-3001 Leuven, Belgium, and Laboratory of Solid State Physics and Magnetism, Katholieke Universiteit Leuven, Celestijnenlaan 200D, B-3001 Heverlee, Belgium

Received May 4, 2006. Revised Manuscript Received June 27, 2006

The development of printed and flexible (opto)electronics requires specific materials for the device's electrodes. Those materials must satisfy a combination of properties. They must be electrically conducting, transparent, printable, and flexible. The conducting polymer poly(3,4-ethylenedioxythiophene)–poly(styrenesulfonate) (PEDOT–PSS) is known as a promising candidate. Its conductivity can be increased by 3 orders of magnitude by the secondary dopant diethylene glycol (DEG). This “secondary doping” phenomenon is clarified in a combined photoelectron spectroscopy and scanning probe microscopy investigation. PEDOT–PSS appears to form a three-dimensional conducting network explaining the improvement of its electrical property upon addition of DEG. Polymer light emitting diodes are successfully fabricated using the transparent plastic PEDOT–PSS electrodes instead of the traditionally used indium tin oxide.

## 1. Introduction

Due to the developments in the area of flexible electronic systems, novel daily life applications are expected to emerge, for instance, sensors or timers printed on goods, electronic newspapers, and wearable electronic devices and displays. Many of those forthcoming applications require low-cost production and flexible electrodes. Promising candidates for electrodes are conducting polymers, such as poly(3,4-ethylenedioxythiophene), or PEDOT. PEDOT was found to be almost transparent and highly stable in thin oxidized films.<sup>1–4</sup> EDOT can be chemically polymerized in a poly(styrenesulfonic acid) (PSS) solution to give a PEDOT–PSS water emulsion.<sup>5</sup> The conjugated polymer PEDOT is positively doped, and the sulfonate anionic groups of PSS are the counterions used to balance the doping charges. PEDOT–PSS films after secondary doping with some inert solvents, such as sorbitol,<sup>6,7</sup> *N*-methylpyrrolidone,<sup>8</sup> (poly)-ethylene glycol and other alcohols,<sup>9–11</sup> dimethyl sulfoxide

(DMSO), *N,N*-dimethylformamide, and tetrahydrofuran,<sup>12</sup> undergo a conductivity increase of 2–3 orders of magnitudes to reach up to 80 S/cm. For the sake of comparison, the conductivity of optimized indium tin oxide (ITO) thin films can reach up to 10<sup>4</sup> S/cm.<sup>13a</sup> After secondary doping, the electrical conductivity of this transparent conducting polymer is sufficient to use it as an electrode in organic electronics.<sup>11</sup> A secondary dopant is an apparently “inert” substance, including a further increase in conductivity of a primarily doped conjugated polymer. It differs from a primary dopant in that the newly enhanced properties may persist even upon complete removal of the secondary dopant. This effect has been first observed with polyaniline derivatives.<sup>13b</sup> The improved performance of PEDOT–PSS together with patterning and printing techniques<sup>14–16</sup> have been successively used in the design of field-effect transistors,<sup>17–19</sup> light-

\* Corresponding author. Telephone: +46 (0)11 36 34 85. Fax: +46 (0)11 36 32 70. E-mail: xavcr@itn.liu.se.

<sup>†</sup> Department of Science and Technology, Linköping University.

<sup>‡</sup> Department of Physics and Measurement Technology, Linköping University.

<sup>§</sup> Division of Molecular and NanoMaterials, Katholieke Universiteit Leuven.

<sup>||</sup> Laboratory of Solid State Physics and Magnetism, Katholieke Universiteit Leuven.

(1) Heywang, G.; Jonas, F. *Adv. Mater.* **1992**, *4*, 116.

(2) Dietrich, M.; Heinze, J.; Heywang, G.; Jonas, F. *J. Electroanal. Chem.* **1994**, *369*, 87.

(3) Winter, I.; Reese, C.; Hormes, J.; Heywang, G.; Jonas, F. *Chem. Phys.* **1995**, *194*, 207.

(4) Pei, Q.; Zuccarello, G.; Ahlskog, M.; Inganäs, O. *Polymer* **1994**, *35*, 1347.

(5) Groenendaal, L.; Jonas, F.; Freitag, D.; Pielartzik, H.; Reynolds, J. R. *Adv. Mater.* **2000**, *12*, 481.

(6) Jönsson, S. K. M.; Birgersson, J.; Crispin, X.; Greczynski, G.; Osikowicz, W.; Gon, A. W. D. v. d.; Salaneck, W. R.; Fahlman, M. *Synth. Met.* **2003**, *139*, 1.

(7) Timpanaro, S.; Kemerink, M.; Touwslager, F.; Kok, M. M. D.; Schrader, S. *Chem. Phys. Lett.* **2004**, *394*, 339.

(8) Louwet, F.; Groenendaal, L.; Dhaen, J.; Manca, J.; Luppen, J. v.; Verdonck, E.; Leenders, L. *Synth. Met.* **1993**, *135–136*, 115.

(9) Crispin, X.; Marciniak, S.; Osikowicz, W.; Zotti, G.; Gon, A. W. D. v. d.; Louwet, F.; Fahlman, M.; Groenendaal, L.; Schryver, F. D.; Salaneck, W. R. *J. Polym. Sci., Part B: Polym. Phys.* **2003**, *41*, 2561.

(10) Wang, T. J.; Qi, Y. Q.; Xu, J. K.; Hu, X. J.; Chen, P. *Appl. Surf. Sci.* **2005**, *250*, 18.

(11) Ouyang, B. Y.; Chi, C. W.; Chen, F. C.; Xu, Q.; Yang, Y. *Adv. Funct. Mater.* **2005**, *15*, 203.

(12) Kim, J. Y.; Jung, J. H.; Lee, D. E.; Joo, J. *Synth. Met.* **2002**, *126*, 311.

(13) (a) Granqvist, C. G.; Hultaker, A. *Thin Solid Films* **2002**, *411*, 1. (b) MacDiarmid, A. G.; Epstein, A. J. *Synth. Met.* **1994**, *65*, 103.

(14) Service, R. F. *Science* **1997**, *278*, 383.

emitting diodes,<sup>11,20</sup> and photovoltaic cells.<sup>21,22</sup> Nowadays, the use of solvent to improve the conductivity of PEDOT–PSS electrodes is an important issue for ink-jet printed electrodes for plastic field effect transistors.<sup>23,24</sup>

Although many studies reported and used the conductivity increase of PEDOT–PSS, the origin of the conductivity increase by those secondary dopants is still unclear. After checking that the doping level is not changed upon addition of DMSO and other solvents, Kim et al. have shown that the PEDOT–PSS sample with DMSO is almost in the critical regime of electrical conduction, which is at the boundary between metallic and insulating states, while the pristine PEDOT/PSS sample is in the insulating regime.<sup>12</sup> They attributed the increase in conductivity to a reduction of the Coulombic interaction between the charge carriers transported on the PEDOT chains and the negative PSS counterions by a screening effect of the polar solvents.<sup>25</sup> Using Raman spectroscopy, Ouyang et al. proposed that the conductivity enhancement of PEDOT–PSS with ethylene glycol, *meso*-erythritol, tetrahydroxybutane, and 2-nitroethanol is due to the conformational change of the PEDOT chains. The driving force is the interaction between the dipoles of the secondary solvent and dipoles or charges on the PEDOT chains.<sup>11</sup> Our preliminary X-ray photoelectron spectroscopy (XPS) studies indicated that sorbitol and diethylene glycol induce a morphology change at the surface of PEDOT–PSS. This was tentatively interpreted as a segregation of the excess PSS.<sup>6,9</sup> However no clear connection was done between the topography of the film and XPS measurements. Timpanaro et al.<sup>7</sup> have shown with scanning tunneling microscopy that the addition of sorbitol leads to an increase in the apparent size of the PEDOT-rich particles, which is associated with the increase of conductivity. Hence, the morphology change within the PEDOT–PSS appears to be another plausible mechanism to explain the high conductivity of PEDOT–PSS.

Here, we present tapping mode atomic force microscopy (AFM) and X-ray and ultraviolet photoelectron spectroscopy measurements performed on thin PEDOT–PSS films to understand the electrical conductivity increase following the addition of diethylene glycol (DEG) in the conducting polymer emulsion. Organic light emitting diodes are fabricated to demonstrate that DEG-modified PEDOT–PSS can

be used as a transparent plastic electrode for flexible electronics.

## 2. Experimental Section

**2.1. Materials.** The chemically prepared PEDOT–PSS is a water emulsion, sodium free (<0.5 ppm), provided by Agfa Gevaert N. V. The PSS-to-PEDOT ratio of this particular emulsion is equal to 2.5. The PEDOT–PSS emulsion contains 1.1 wt % PEDOT–PSS. A defined amount of DEG is added into the emulsion.

**2.2. Instrumentation.** X-ray photoelectron spectroscopy, originally known as electron spectroscopy for chemical application (ESCA), is carried out using a Scienta ESCA200 spectrometer with a base pressure of  $2 \times 10^{-10}$  mbar (ultrahigh vacuum) and monochromatized Al K $\alpha$  radiation ( $h\nu = 1486.6$  eV). The binding energy of the gold Au(4f<sub>7/2</sub>) line is calibrated to 83.9 eV. The experimental conditions are such that the full width at half-maximum (fwhm) of the gold Au(4f<sub>7/2</sub>) line is 0.65 eV. The S(2p) signal of PEDOT/PSS is a doublet S(p<sub>1/2,3/2</sub>), due to the spin–orbit coupling. The ultraviolet photoelectron spectroscopy (UPS) measurements are carried out with a spectrometer of our own design and construction, with a base pressure less than  $1 \times 10^{-9}$  mbar. The UPS spectra are recorded using monochromatized HeI (21.2 eV) and HeII (40.8 eV) radiations from a helium discharge lamp. On the basis of the width of the gold Fermi edge, the energy resolution is about  $\pm 0.1$  eV.

Tapping mode and simultaneously acquired phase images are obtained with a DI-Multimode AFM (Veeco Instr.), connected to a Nanoscope IV controller (Veeco) in combination with a SAMIII (Signal Access Module, Veeco). TAP300A AFM tips with an approximate resonant frequency of 300 kHz (Lot-Oriel) are used for the tapping-mode measurements.

**2.3 Polymer Diodes.** Polymer-based light emitting diodes (p-LEDs) are fabricated with the anode consisting of PEDOT–PSS with or without DEG spin cast on glass slides. To prevent aggregations, the PEDOT–PSS suspension is first treated in an ultrasonic bath at 50 °C for 15 min. To further reduce the number of aggregates, the solution is filtered in a 1.0  $\mu$ m membrane filter. To ensure proper adhesion, a layer of PEDOT–PSS with 0.2 wt % Silquest (Bayer A-187) and zonyl (Fluka FS-300) is first spin-coated at 2000 rpm for 30 s on top of the clean glass slides. On top of this adhesion layer, either pure PEDOT–PSS or PEDOT–PSS with 5 wt % DEG is spin-coated at 2000 rpm for 30 s. Each layer is dried in an oven at 120 °C for 5 min prior to deposition of the next layer. Devices are defined by patterning the PEDOT–PSS layers using NaOCl for 10 s following copious rinsing in DI water and drying in an oven at 120 °C for 5 min. The conjugated polymer poly[2-methoxy-5-(2-ethylhexyloxy)-1,4-phenylenevinylene], so-called MeH–PPV, is dissolved in CHCl<sub>3</sub> (7.5 mg/mL) and spin-coated at 1000 rpm for 15 s on top of PEDOT–PSS with or without DEG. To complete the device structure, aluminum top electrodes are deposited through a shadow mask using vacuum deposition at a pressure of  $5 \times 10^{-6}$  Torr. To ensure low contact resistance between the probe and the PEDOT–PSS layer, contacts are painted onto the bare PEDOT–PSS using silver paste.

## 3. Results and Discussion

**3.1. Electrical Conductivity.** The evolution of the film conductivity (measured by four-point probe techniques) versus the percentage in weight of DEG added to the PEDOT–PSS emulsion (41 wt % of a 1.1 wt % PEDOT–PSS dispersion free of sodium, 48–58 wt % water, and 0–10 wt % DEG) is reported in Figure 1. The films have been

- (15) Granlund, T.; Nyberg, T.; Roman, L. S.; Svensson, M.; Inganäs, O. *Adv. Mater.* **2000**, *12*, 269.
- (16) Stutzmann, N.; Tervoort, T. A.; Broer, D. J.; Siringhaus, H.; Friend, R. H.; Smith, P. *Adv. Funct. Mater.* **2002**, *12*, 105.
- (17) Siringhaus, H.; Kawase, T.; Friend, R. H.; Shimoda, T.; Inbasekaran, M.; Wu, W.; Woo, E. P. *Science* **2000**, *290*, 2123.
- (18) Lu, J.; Pinto, N. J.; MacDiarmid, A. G. *J. Appl. Phys.* **2002**, *92*, 6033.
- (19) Wang, J. Z.; Zheng, Z. H.; Li, H. W.; Huck, W. T. S.; Siringhaus, H. *Nat. Mater.* **2004**, *3*, 171.
- (20) Kim, W. H.; Mäkinen, A. J.; Nikolov, N.; Shashidhar, R.; Kim, H.; Kafafi, Z. H. *Appl. Phys. Lett.* **2002**, *80*, 3844.
- (21) Arias, A. C.; Granström, M.; Pertritsch, K.; Friend, R. H. *Synth. Met.* **1999**, *102*, 953.
- (22) Kushto, G. P.; Kim, W. H.; Kafafi, Z. H. *Appl. Phys. Lett.* **2005**, *86*, 093502.
- (23) Xue, F.; Su, Y.; Varshneyan, K. *IEEE Trans. Electron Devices* **2005**, *52*, 1982.
- (24) Lim, J. A.; Cho, J. H.; Park, Y. D.; Kim, D. H.; Hwang, M.; Cho, K. *Appl. Phys. Lett.* **2006**, *88*, 082102.
- (25) Lee, C. S.; Kim, J. K.; Lee, D. E.; Koo, Y. K.; Joo, J.; Han, S.; Beag, Y. W.; Koh, S. K. *Synth. Met.* **2003**, *135*, 13.

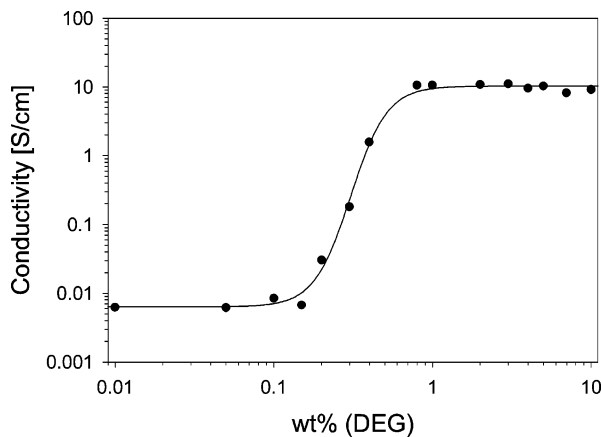


**Figure 1.** log of the electrical conductivity (four-point probe measurements) in thin films versus the amount of DEG (wt %) introduced in the PEDOT-PSS water emulsion.

spin-coated on quartz substrates and dried at room temperature. The film thickness estimated from profilometer (Dektak) measurements is about 100 nm. The logarithm of the conductivity,  $\sigma$ , is reported versus the logarithm of the weight percent of DEG added in the emulsion.  $\log(\sigma)$  displays a sigmoid evolution. The conductivity of pristine PEDOT-PSS is about  $0.006 \text{ S cm}^{-1}$  and suddenly increases to  $10 \text{ S cm}^{-1}$  at a specific concentration of DEG ( $\approx 0.3 \text{ wt } \%$ ). The sharp conductivity increase strongly indicates that the origin is not a screening effect of the interaction between ions and charge carriers by the solvent, which would be progressive, but rather a phase separation.

To investigate if and how phase separation occurs, several techniques are used to characterize the film surface. We characterize the morphology of the surface rather than the bulk morphology because bulk techniques are not very sensitive to disorder polymer blends composed of two materials close in nature, the two polymers PEDOT and PSS.

**3.2. Surface Morphology.** The morphology of PEDOT-PSS films without DEG and with 5 wt % of DEG is characterized with tapping-mode AFM. The polymer films are cast on gold substrates. Figure 2A shows the topography of a  $1 \times 1 \mu\text{m}^2$  area of the PEDOT-PSS film without DEG. Grains and some elongated structures of a dimension of about 20–30 nm are observed on the surface of these films (see Figure 2A,C). In the corresponding tapping-mode phase images (Figure 2B,D), the low contrast in the phase image (full scale equals  $10^\circ$ ) is likely induced by the topographic variations. Figure 3A shows the topography of the PEDOT-PSS film with DEG. Particles can be observed on the film surface, as well as some elongated features. The simultaneously acquired phase image (see Figure 3B) displays bright and dark regions. After enlarging the image, the dark regions in Figure 3D (phase image) correspond to small islands in Figure 3C (topography image), which are irregular in shape, seldom circular, and mostly elongated. Their typical dimension is on the order of 20 nm. The strong contrast at the border of the small islands in the phase image (full scale equals  $45^\circ$ ; see Figure 3D) is associated with a different chemical composition of the small islands compared to the surrounding matrix. For polymer systems, a lower phase angle means a softer material, whereas a higher phase angle can be identified with a harder material. In general, attribution

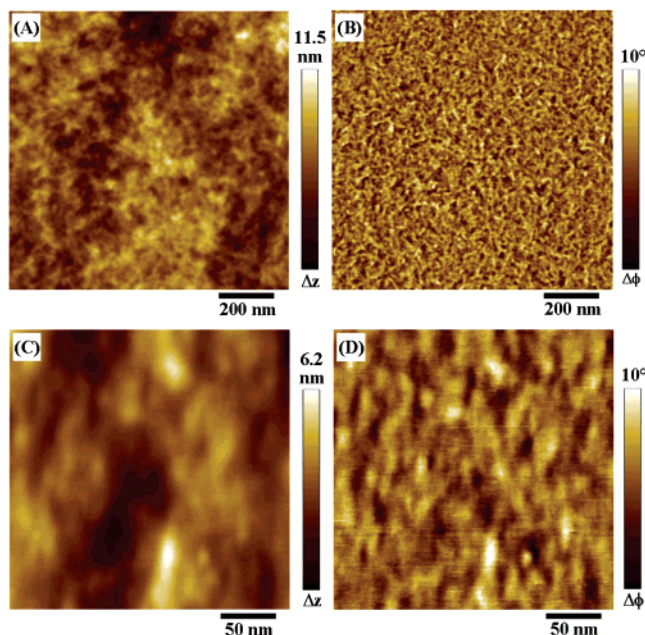


**Figure 2.** Topography (A, C) and phase images (B, D) of a pure PEDOT-PSS film (without added solvents) obtained with tapping-mode AFM at a scale of  $1 \times 1$  and  $0.25 \times 0.25 \mu\text{m}^2$ .

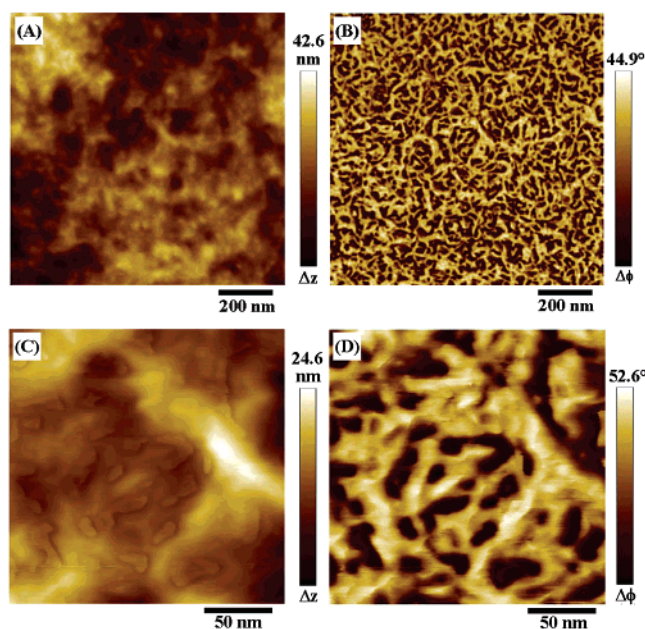


**Figure 3.** Topography (A, C) and phase images (B, D) of a PEDOT-PSS film with 5 wt % added DEG obtained with tapping-mode AFM at a scale of  $1 \times 1$  and  $0.20 \times 0.20 \mu\text{m}^2$ .

of different materials from tapping-mode AFM images is not straightforward, since the phase image signal is determined by several factors such as the amplitude setpoint, tip indentation, surface forces, and bulk properties (elasticity/viscoelasticity). For polymer systems, with phase images captured under moderate tapping conditions, bright areas in the phase image can be assigned to a relatively hard phase.<sup>26</sup> This means that the regions showing a lower phase signal in Figure 3D correspond to a relatively soft material with respect to the surroundings. The regions or islands in Figure 3C are attributed to excess PSS material. Surface areas

(26) Wang, Y.; Song, R.; Li, Y.; Shen, J. *Surf. Sci.* **2003**, *530*, 136.

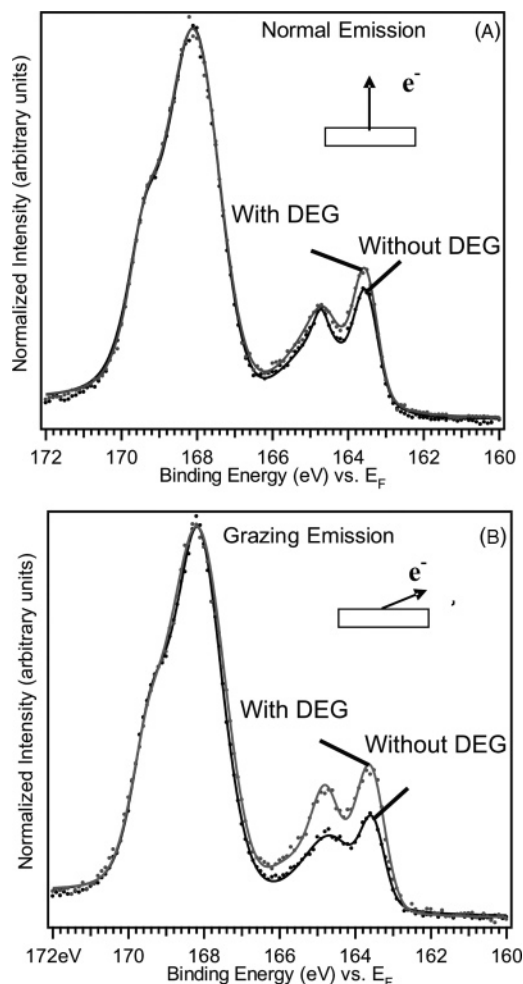


**Figure 4.** XPS S(2p) spectra of PEDOT–PSS films with 5 wt % DEG and without DEG in “normal emission” (A) and in “grazing emission” (B). In the grazing emission mode, electrons are collected at a grazing angle relative to the sample surface. This mode is more sensitive to the surface of the sample. The observed PEDOT-to-PSS ratio increases upon the addition of DEG.

rich in this hygroscopic polyelectrolyte are expected to swell and soften due to ambient humidity and/or the added DEG. The added secondary dopant DEG thus induces a phase separation on the nanometer scale characterized by a segregation of the excess PSS in domains surrounded by a PEDOT–PSS phase.

**3.3. Surface Composition via XPS.** To strengthen the interpretation of the AFM images, XPS measurements are performed on these films. XPS is a surface-sensitive technique, but with no lateral resolution, since the size of the analyzed spot is about a few  $\text{mm}^2$ . Hence XPS appears complementary to AFM techniques. Both PEDOT and PSS contain one sulfur atom per repeat unit. The sulfur atom in PEDOT is within the thiophene ring, whereas in PSS it is included in the sulfonate moiety. Due to those different chemical environments, the S(2p) electrons of PEDOT and PSS have different binding energies so that the composition of PEDOT–PSS can be analyzed by XPS.<sup>27</sup> The S(2p) XPS spectrum displays two contributions (see Figure 4). The sulfur signal for PSS appears at higher binding energy (168.8

eV) due to the three electronegative oxygen atoms withdrawing the electron density of the sulfur atom. The S(2p) doublet at 164.2 eV comes from PEDOT. The XPS S(2p) spectra of PEDOT–PSS films gives directly the surface sulfonate–thiophene ratio ( $R_{S/T}$ ) equivalent to the surface PSS/PEDOT ratio. Figure 4A shows the S(2p) signal for PEDOT–PSS films with (gray line) and without (black line) DEG. In this experiment, the photoelectrons are collected normal to the surface. The probing depth of the spectroscopy is defined by the inelastic mean free path of the S(2p) photoelectrons, i.e. about 140 Å for a kinetic energy of 1320 eV.<sup>28</sup> Upon adding DEG, the amount of PEDOT probed increases by less than 10%. For this probing depth, the average surface composition is almost not changed. Note that similar negligible changes in the S(2p) spectra of PEDOT–PSS upon the addition of a secondary dopant have also been observed by others.<sup>10,12</sup>

To shed light on the relationship between the composition and the morphology of PEDOT–PSS, the geometry of the XPS experiment is modified. The polymer films are characterized at higher electron-emission angle ( $\theta = 80^\circ$ ) defined with respect to the surface normal (Figure 4B). Collecting the photoelectrons at this grazing angle strongly increases the surface sensitivity of the experiment. The addition of DEG is accompanied with an increase of 45% of the PEDOT S(2p) signal due to the morphology and surface composition change. The correlation between the XPS data and the AFM phase and topography images (Figures 2 and 3) is a priori not obvious and requires a closer look. Therefore some cross-sectional profiles of the AFM topography and phase images, together with the (calculated) XPS probing depth at each position, are presented in Figure 5. The full lines in Figure 5A,B illustrate typical topography profiles along a line measured on the sample without DEG and with DEG, respectively. The dotted lines represent the value of the phase for both samples. On the basis of the observed topography profile, in combination with the known probing depth defined by the inelastic mean free path of the S(2p) photoelectrons, it is possible to calculate the XPS probing depth at each coordinate. The dashed lines define the depth profile probed with XPS ( $\theta = 80^\circ$ ). The difference between the topography profile (full line) and the XPS depth profile (dashed line) defines the depth probed with XPS, which is illustrated by the full line in Figure 5C. Negative regions for the sample with DEG represent invisible regions for XPS. Without DEG, the surface is flatter and the overall surface area contributes to the XPS signal. A number of observations can be made upon close examination of typical profiles displayed in Figure 5A,B. First of all, in Figure 5A, the topography and the phase profile show a one-to-one correspondence. The top of each small bump or grain is associated with a higher value of the phase, meaning that the (rather small) variations of the phase signal are induced by the small topographic variations. This is in contrast with the phase signal of the sample with the added DEG, where this one-to-one correspondence of sample topography and phase signal has clearly diminished and is absent in some parts of the profile. On top of the small islands visible in Figure 3C, the phase signal is much lower than

(27) Zotti, G.; Zecchin, S.; Schiavon, G.; Louwet, F.; Groenendaal, L.; Crispin, X.; Osikowicz, W.; Salaneck, W.; Fahlman, M. *Macromolecules* **2003**, *36*, 3337.

(28) Cartier, E.; Pfüger, P.; Pireaux, J.-J.; Vilar, M. R. *Appl. Phys.* **1987**, *A 44*, 43.

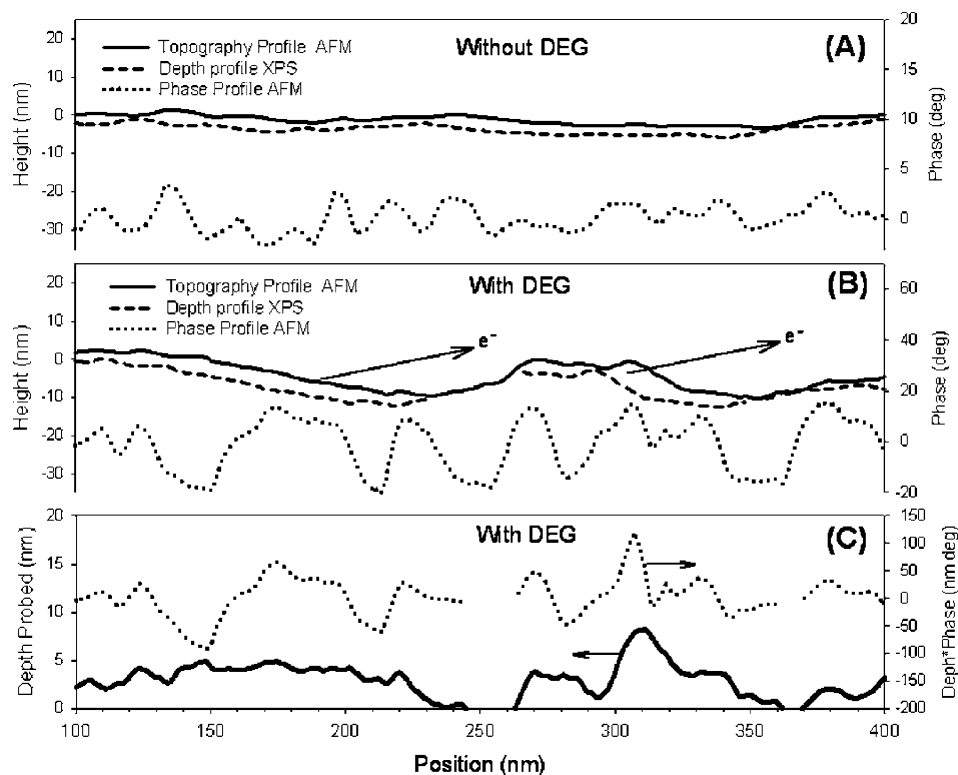


**Figure 5.** AFM topography profile (full line), AFM tapping-mode phase profile (dotted line), and the calculated XPS probing profile for grazing angle ( $\theta = 80^\circ$ ) XPS experiments on PEDOT-PSS films without (A) and with (B) added DEG. (C) Profile of the quantity  $Q$  (dotted line), defined by the product of the XPS probing depth (full line) and the phase angle (dotted line in B).

the surrounding regions, although the topographic variations associated with these islands are minor. As stated above, this is due to the occurrence of a phase separation on the sample surface.

The calculated XPS probing depth profiles explain well the overall XPS spectra. For the sample without DEG, the topographic variations are shallow and XPS probes the entire surface of the sample in both bulk (normal emission) and surface sensitive (grazing emission; see Figure 5A) XPS detection mode. The photoelectrons detected at grazing angle emission originate from the material present between the surface defined by the topography profile (solid line) and the XPS depth profile (dashed line). For the sample with DEG (Figure 5B), it can be clearly seen that, due to the larger height variations in topography, in some regions the XPS probing depth is minimal or even equals zero. This means that photoelectrons from some regions cannot reach the detector due to the scattering in neighboring grains. These regions can be identified as the PSS regions possessing a low phase signal. This corroborates well with the XPS spectrum since the overall PEDOT-to-PSS ratio increases upon the addition of DEG. A quantity  $Q$  can be defined, which is given by the product of the phase angle and the depth probed by XPS. A good indication for the composition is given by the phase angle, since low-phase regions can be identified with PSS and the higher phase regions with PEDOT-PSS. Hence, the quantity  $Q$  illustrates if XPS at grazing angle sees more of the phase of the blend with a high phase angle or the opposite. The profile of that quantity (in nm deg) is displayed as the dotted line in Figure 5C. For instance, at 310 nm, XPS probes the sample within a depth of 7 nm under the surface. At the same position, the phase

angle is large (Figure 5A); thus  $Q$  is also large, meaning that this position is more visible with the XPS at grazing angle and it is related to a white spot in the phase image. The average value of  $Q$  over a long line (1  $\mu\text{m}$ ) on the sample is about 5 for the sample with DEG, while it is equal to zero without DEG. Hence, with DEG, the rigid domains (larger phase angle) should contribute more to the XPS signal (Figure 4B). The correlation between XPS and AFM indicates that the domains with a large phase angle in the phase image are rich in PEDOT; consequently they are the PEDOT-PSS domains, while the negative phase angle are associated with the demixed PSS phase.

**3.4. Valence Electronic Levels at the Surface.** UPS ( $h\nu = 21.2$  eV) is a very sensitive technique with a probing depth of just a few angstroms. This is a complementary technique to XPS to characterize the surface composition of PEDOT-PSS films. The UPS spectra of PEDOT-PSS with and without DEG, as well as two reference materials, PEDOT-tosylate (PEDOT-Tos) and PSS, are reported in Figure 6. PEDOT-Tos, synthesized by vapor-phase polymerization,<sup>29</sup> has a high content of PEDOT ( $R_{ST} = 0.28$  estimated from XPS). The high density of conducting polymer explains the high electrical conductivity ( $\sim 800$  S/cm) measured for those films. Consequently, most of the signal in the UPS spectrum of PEDOT-Tos (dashed line) arises from the electronic levels of positively doped PEDOT. Compared to the UPS spectrum of PSS (full line), an insulating material, PEDOT-Tos has a significant density of state in the low binding energy region (5–6 eV vs vacuum level) that originates from doping levels of the PEDOT chains; PSS has no density of

(29) Winther-Jensen, B.; West, K. *Macromolecules* **2004**, *37*, 4538.

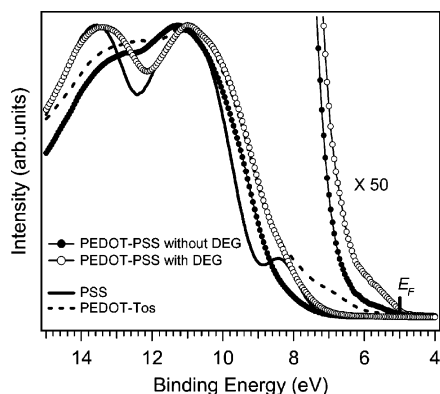


**Figure 6.** UPS valence band spectra (HeI radiation) of PEDOT/PSS without and with 5 wt % DEG (black and white dots, respectively). The zoom (times 50) of the low binding energy area is displayed on the right-hand side. Solid lines in black and gray shows reference measurements on PSS and PEDOT–Tos, respectively. The binding energy is relative to the vacuum level determined from the work function of the samples. The work function of PSS is 5.5 eV, PEDOT–Tos is 4.4 eV, and PEDOT–PSS with and without DEG is 5.0 eV.

state in that region. The reference sample PEDOT–Tos has 8 times more PEDOT than in a PEDOT–PSS film with DEG. Interestingly the density of states at low binding energies (5–6 eV) in PEDOT–Tos is also 8 times higher than in the sample with DEG. This low binding energy region reveals the surface content in PEDOT and appears as an essential feature to understand the surface composition change when DEG is added in the PEDOT–PSS emulsion.

PEDOT–PSS with or without DEG have the same work function ( $WF = 5.0$  eV). PEDOT–PSS, with or without DEG, behave like metals in terms of electrical contact since their Fermi levels align with that of the spectrometer. In the UPS spectrum using the vacuum level as a reference level, the density of state drops at 5.0 eV (WF), corresponding to the Fermi level of the polymer layers. In the range between 5 and 6 eV, PEDOT–PSS films with DEG (white circles) have three times larger density of state at low binding energy compared to the film without DEG (black circles). This supports the AFM phase image, which indicates that the top surface of PEDOT–PSS without DEG contains more PSS as indicated by the narrow range in phase angle (see Figure 3). In contrast, the presence of DEG is such that the excess of PSS is phase-segregated in domains leaving doped PEDOT-rich domains visible at low binding energies in the UPS spectrum. According to that model, the morphology change due to presence of DEG does not only increase by 3 orders of magnitude the conductivity, but it also increases the effective area, rich in PEDOT, for charge injection for a PEDOT–PSS electrode in a device.

**3.5. Proposed Mechanism for the Secondary Dopant Effect in PEDOT–PSS.** The relationship between the conductivity, the surface composition, and the morphology can be explained from the distribution of the PSS in excess in the films. Without DEG, the conducting PEDOT–PSS grains are covered with a very thin layer of the insulating PSS material,<sup>9,30</sup> such that the polymer blends look like conducting grains in a PSS matrix. Upon addition of DEG, the excess PSS is phase-segregated into PSS-rich, insulating

domains, while highly conducting PEDOT–PSS grains merge together to form a three-dimensional conducting network. Note that the conductivity of PEDOT–PSS with DEG ( $10 \text{ S cm}^{-1}$ ), with a large excess of PSS ( $R_{S/T} \approx 4$ ), is of the same order of magnitude as the conductivity of electropolymerized PEDOT–PSS films ( $80 \text{ S cm}^{-1}$ ) containing more PEDOT than PSS ( $R_{S/T} = 0.7$ ).<sup>27</sup> This suggests that the chemical composition of PEDOT–PSS in the three-dimensional network, obtained upon adding DEG, might be close to the electropolymerized PEDOT–PSS.

Our XPS and AFM analyses appear complementary to Raman spectroscopy investigation by Ouyang et al.<sup>11</sup> In their study, the authors associate the conductivity enhancement of PEDOT–PSS to the conformational change of the PEDOT chains. This explains at a microscopic level what happens to the PEDOT chains after phase separation. It is indeed likely that the PEDOT chains in the formed three-dimensional conducting network reorganize at the microscopic level either by changing shape, such as that found with polyaniline,<sup>13,31,32</sup> and/or improving the interchain packing thanks to  $\pi$ – $\pi$  interaction stabilizing the system (such as that found in PEDOT–Tos<sup>33,34</sup>).  $\pi$ – $\pi$  stacking between conjugated polymer chains is known to lead to charge mobility improvement.<sup>35</sup>

Although, the reason for the large conductivity of PEDOT–PSS with DEG seems clear from our study, the mechanism leading to this phase separation is still unknown. We propose the following explanation. During the polymerization of EDOT monomers with an oxidant in a PSS–water solution, PEDOT chains are formed.<sup>5,27</sup> However, a stable PEDOT–PSS emulsion is only obtained upon vigorous shaking of the reaction vessel to increase the contact area between two phases, PSS–water solution and PEDOT–PSS assemblies, and lead to PEDOT–PSS particles in the water–PSS solution. In this process the mechanical energy is transformed into interfacial energy between the two phases, such that the stable emulsion is characterized by a positive Gibbs energy (including entropic and enthalpic variations). Spin coating such an emulsion on a substrate would lead to a film composed of PEDOT–PSS particles surrounded by the excess PSS.<sup>30</sup> The particles are barely touching each other such that the overall electrical conductivity is relatively low.

We believe that part of the positive Gibbs energy, stored in the emulsion, can be released upon the addition of DEG, thus leading to a phase separation between the excess PSS and PEDOT–PSS (doped PEDOT and PSS chains are electrostatically bound). The phase separation is expected to occur during the drying process and not directly in the emulsion. Indeed, when adding a few weight percent of the highly soluble DEG in the water emulsion (Henry’s law constant  $k_H = 4 \times 10^6 \text{ M/atm}$ ), most of the DEG molecules stay in water. However, upon water evaporation, the high

(30) Greczynski, G.; Kugler, T.; Keil, M.; Osikowicz, W.; Fahlman, M.; Salaneck, W. R. *J. Electron Spectrosc., Relat. Phenom.* **2001**, *121*, 1.

(31) Joo, J.; Chung, Y. C.; Song, H. G.; Baeck, J. S.; Lee, W. P.; Epstein, A. J.; MacDiarmid, A. G.; Jeong, S. K.; Oh, E. J. *Synth. Met.* **1997**, *84*, 739.

(32) Rannou, P.; A.Pron; Nechtschein, M. *Synth. Met.* **1999**, *101*, 827.

(33) Aasmundtveit, K. E.; Samuelsen, E. J.; Pettersson, L. A. A.; Inganäs, O.; Johansson, T.; Feidenhans, R. *Synth. Met.* **1999**, *101*, 561.

(34) Kim, T. Y.; Park, C. M.; Kim, J. E.; Suh, K. S. *Synth. Met.* **2005**, *149*, 169.

(35) Brédas, J. L.; Calbert, J. P.; Filho, D. A. d. S.; Cornil, J. *Proc. Natl. Acad. Sci. U.S.A.* **2002**, *99*, 5804.

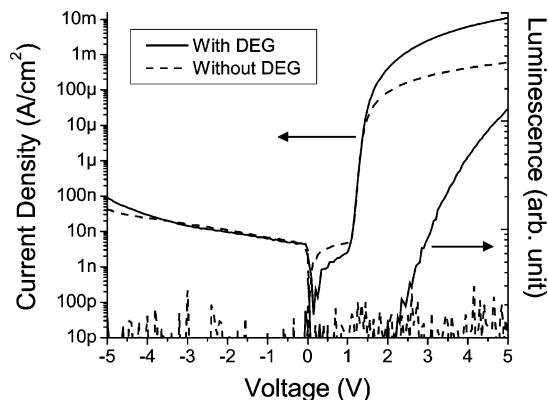


**Figure 7.** Current density–voltage characteristics of polymer diodes using PEDOT–PSS with 5 wt % DEG (full line) and without DEG (dashed line) as an electrode. The polymer light emitting diode has the following structure: PEDOT–PSS/MEH–PPV/Al.

boiling point solvent DEG ( $T_{\text{boiling}} = 244\text{ }^{\circ}\text{C}$ ) evaporates much more slowly such that it reaches a higher concentration in the remaining PEDOT–PSS wet films. DEG can eventually swell PSS-rich regions and screen the long-range electrostatic interactions, holding the excess PSS attached to the PEDOT–PSS. For a specific threshold of concentration (see Figure 1), the amount of DEG in the wet film is enough to lead to a phase separation of the excess PSS chains from the PEDOT–PSS chain assemblies, thus creating the three-dimensional conducting network. This proposed hypothesis explains the conductivity data by Kim et al., which reveal that the highest conductivity for PEDOT–PSS is obtained with the solvent of highest dielectric constant (electrostatic interactions inversely proportional to the dielectric constant).<sup>12</sup> In summary, several properties are required for the secondary dopants for PEDOT–PSS: high solubility in water, high boiling point, and high dielectric constant.

**3.6. PEDOT–PSS Electrodes in a Polymer Light Emitting Diode.** Polymer light emitting diodes (p-LEDs) are fabricated with the anode consisting of PEDOT–PSS with or without DEG spin cast on glass slides. The transparent plastic electrodes are coated with the emitting polymer MEH–PPV. Aluminum(oxide) is used as electron injecting electrode. Figure 7 shows the current density–voltage ( $J$ – $V$ ) characteristics of the p-LED's with or without DEG in the PEDOT–PSS bottom electrode. Both types of devices show a very clear injection behavior, with an exponentially increasing current between 1 and 1.5 V as well as a rectification of 5 orders of magnitudes, which indicates the good quality of the diode. Above 1.5 V the devices without DEG show a linear  $J$ – $V$  behavior, indicating a limitation of the current due to the higher resistance in the PEDOT–PSS electrode. Devices with DEG do not show any sign of limitation of this kind. On the contrary, these devices show typical space charge limited current ( $J$ – $V^2$ ) at voltages exceeding 2 V, indicating that the mobility of the MEH–PPV layer is the limiting factor for the current. The devices with DEG show an onset of luminescence near 2 V, while

the devices without DEG do not show any light within the voltage range in this experiment. We believe this is because the hole current from the PEDOT–PSS electrode never reaches a high enough level.

#### 4. Conclusions

We have employed noncontact AFM, XPS, and EFM to investigate the origin of the conductivity increase of PEDOT–PSS when adding diethylene glycol to the emulsion. The conductivity of pristine PEDOT–PSS films increases from 0.006 to 10 S  $\text{cm}^{-1}$ . The secondary dopant effect of DEG is associated with the phase separation observed with AFM. Small islands with a very distinct contrast in the non-contact AFM phase signal are attributed to phase-separated PSS. Since the excess PSS is (partly) phase-separated, the effective insulation of the conducting PEDOT–PSS particles by the excess PSS is considerably reduced, leading to better pathways for conduction and an interconnected three-dimensional network of conducting PEDOT–PSS. XPS measurements reveal an increased PEDOT-to-PSS ratio at grazing angle, which is associated with the morphology and composition change at the surface of the film in agreement with the AFM analysis. A mechanism is proposed for the phase separation of the excess PSS from the PEDOT–PSS regions, according to which solvents need to have high solubility in water, high boiling point, and high dielectric constant, to constitute a good secondary dopant for PEDOT–PSS.

The morphology change due to the presence of DEG does not only increase by 3 orders of magnitude the conductivity, but it also increases the effective area, rich in PEDOT, for charge injection for a PEDOT–PSS electrode in a device. This is additionally confirmed by UPS measurements indicating a higher density of states at the Fermi level when adding DEG in the plastic electrode. Polymer diodes, using PEDOT–PSS as plastic electrode, clearly show the impact of DEG on the current density–voltage characteristics. The improvement of the PEDOT–PSS conductivity with DEG allows reaching high current in MEH–PPV, such that electroluminescence is observed. Those results show the potential of DEG-modified PEDOT–PSS electrodes for flexible electronics including plastic solar cells and light emitting diodes.

**Acknowledgment.** Linköping University gratefully acknowledges the Swedish Foundation for Strategic Research (COE@COIN), VINNOVA, The Royal Swedish Academy of Sciences, and The Swedish Research Council for financial support of this project. Katholieke Universiteit Leuven gratefully acknowledges the financial support of IWT (Instituut voor de aanmoediging van Innovatie door Wetenschap en Technologie) through the STWW (Strategische Technologieën voor Welzijn en Welvaart) Project No.156. We thank Agfa Gevaert N.V. (Mortsel, Belgium) for providing us with the PEDOT–PSS material.

CM061032+